Magnetic properties and spin reorientation of hexagonal HoFeO$_3$ thin films

Check for updates

R.C. Rai [*], C. Horvatits, S. Deer

Department of Physics, SUNY Buffalo State, Buffalo, NY 14222, USA

ARTICLE INFO

ABSTRACT

We present structural, magnetic, and optical properties of hexagonal HoFeO$_3$/Al$_2$O$_3$ thin films deposited by Magnetron Sputtering. The x-ray diffraction patterns of HoFeO$_3$ thin films show the c-planes of a hexagonal structure. The magnetization data display an antiferromagnetic transition temperature, T$_N \sim$120 $\pm$ 5 K and the magnetization-field hysteresis loops were measured below 100 K, confirming a weak ferromagnetism arising from a spin canting of the Fe^{3+} moments. The magnetization data also show an anomaly around ~40 K due to a spin-reorientation transition caused by the Ho^{3+}- Fe^{3+} interactions. We observed comparable magnetization along the *ab* plane and *c* axis although the spin canting of Fe^{3+} sites has a preferential component along the *c* axis, suggesting that the Ho^{3+}- Fe^{3+} interactions dominate in the low temperature magnetic structures of hexagonal-HoFeO$_3$. The observed electronic excitations at ~2.29, 2.87, 3.82, 4.79, and 6.53 eV have been assigned to the Fe^{3+} *d* to *d* on-site as well as O 2*p* to Fe 3*d*, Ho 6*s*, and 5*d* charge-transfer excitations, respectively. The room temperature energy band gap of the hexagonal-HoFeO$_3$ thin film was measured to be ~1.99 $\pm$ 0.04 eV.

1. Introduction

Hexagonal HoFeO$_3$ belongs to the RFeO$_3$ (R = Dy-Lu) family, which are commonly found in the orthorhombic structure. This family of bulk orthoferrites can be stabilized in a metastable hexagonal structure (P6$_3$cm) in a thin film form by depositing onto hexagonal substrates, such as *c* axis Al$_2$O$_3$ and (111) yttrium-stablized zirconia (ysz) [1–10]. Interestingly, hexagonal RFeO$_3$ (in short, h-RFeO$_3$) thin films show ferroelectricity at room temperature, driven by a structural distortion [11,12]. In addition, these hexaferrite thin films, depending on the rare-earth ion, undergo an antiferromagnetic transition in the temperature range ~110-185 K [3,4,9–14]. The antiferromagnetic structure of these hexaferrites has a triangular lattice with a canted spin along the *c* axis, resulting in a weak ferromagnetic state [14–16]. Consequently, hexagonal RFeO$_3$ exhibit both ferroelectricity and ferromagnetism in a single phase, and hence these hexaferrites are multiferroics having potential technological applications.

Many members of the RFeO$_3$ family have been successfully stabilized in a hexagonal thin film form and their ferroelectric and magnetic properties have been investigated. For example, there have been reports of thin film fabrications of h-LuFeO$_3$ [7,9,17–19], h-YbFeO$_3$ [3,20–23], h-TmFeO$_3$ [4], and h-ScFeO$_3$ [10,24,25], and their physical properties. Among these hexaferrites, the magnetic transition comes from the long

range ordering of Fe^{3+} spins and a weak ferromagnetism is a result of the Fe^{3+} spin canting along the *c* axis caused by the Dzyaloshinskii-Moriya interaction [4,7,12,14]. Meanwhile, the low temperature magnetic structures are very different among them due to the spin of the rare earth ion (R^{3+}) which varies for each member. For RFeO$_3$ with a magnetic R^{3+} ion, there are three different magnetic interactions in the system, such as Fe^{3+}-Fe^{3+}, Fe^{3+}-R^{3+}, and R^{3+}-R^{3+} resulting in a complex magnetic structure. At low temperature, the magnetic properties of these hexaferrites are strongly dominated by the Fe^{3+}-R^{3+} and R^{3+}-R^{3+} interactions. Due to the Fe^{3+}-R^{3+} interactions, some of these members exhibit a spin reorientation transition below 50 K in which the spins of Fe$^{Fe^{3+}}$ ions reorient in the *ab* plane [3,9,19,25]. While the most members of the RFeO$_3$ family have been extensively studied, there are only a few published reports on h-HoFeO$_3$ thin films [13,26]. Despite the previous works on h-HoFeO$_3$ thin films by Akbashev et al. [13] and Pavlov et al. [26] that have shed light on the magnetic transition temperature and optical properties in the photon energy range of 1.7 - 4.8 eV, the low temperature magnetic properties and the energy band gap of h-HoFeO$_3$ are not explored yet. Because of a large moment of the Ho^{3+} ion, h-HoFeO$_3$ is expected to have a complex magnetic structure at low temperature and its magnetic properties could differ from the other family members. As a result, the study on the low temperature magnetic properties of h-HoFeO$_3$ is desirable. Similarly, the optical properties that

capture the electronic excitations in a wider photon energy range (1 - 6 eV) and the energy band gap of the h-HoFeO$_3$ thin film also need to be explored and compared with the other family members of RFeO$_3$.

In this article, we present the structural, optical, and magnetic properties of h-HoFeO$_3$ thin films, deposited on (001) Al$_2$O$_3$ substrates by radio-frequency (RF) magnetron sputtering. The X-ray diffraction patterns of HoFeO$_3$ thin films confirm a hexagonal structure. The magnetic moment versus temperature curves show a magnetic transition temperature around T$_N$ ~120 ± 5 K. We discuss the low temperature magnetic properties in the context of the interactions between the Ho^{3+} and Fe^{3+} sites. The moment-field hysteresis loops have also been observed below 100 K, indicating a weak ferromagnetism due to spin canting. Based on the room temperature optical properties of the h-HoFeO$_3$ thin film, the observed electronic excitations between 2.29 eV and 6.53 eV have been assigned to the Fe^{3+} $d{\to}d$ on-site and O $2p{\to}$Fe $3d$ and O $2p{\to}$Ho $5d$ and $6s$ charge-transfer electronic transitions.

2. Experimental

HoFeO$_3$ was prepared by a conventional solid state reaction by thoroughly mixing a stoichiometric ratio of Ho$_2$O$_3$ and Fe$_2$O$_3$ powder samples in the mortal and pestle. The sample was then pressed into pellets and sintered at 1200 °C for 12 hours. After sintering, the pellets were re-ground and pressed into pellets, and sintered again at 1200 °C for 12 hours. For the deposition of HoFeO$_3$ thin films, one-inch diameter sintered pellet of HoFeO$_3$ was used as a target for an RF magnetron sputtering, which has a confocal, off-axis geometry with the source facing downward to the substrate stage at about 3 inch distance. The single crystal substrates of (001) Al$_2$O$_3$ were ultrasonically cleaned in acetone, ethanol, and deionized water in sequence, and the substrates were mounted on the substrate stage. The deposition chamber was pump down to the base pressure of ~2.7 x 10^{-4} Pa with a turbo-molecular pump. Before the deposition process, the substrates were preheated at 600 °C for 30 min and temperature was gradually increased to the deposition temperature 825 °C. The sputtering gas was argon with a purity of 99.999%. A reactive gas, oxygen (purity of 99.999%), was also inserted into the chamber. The ratio of argon to oxygen was ~9. The sputtering power of 22 Watts was used which yielded the deposition rate of ~12 Å per minute. To improve the sample thickness uniformity, the substrate stage was continuously rotated at 20 revolution per minute during the deposition process. All deposited HoFeO$_3$ thin films (~150 nm thick) were post-deposition annealed in ambient air in a tube furnace at 800 °C for 3 hours.

The surface morphology of the h-HoFeO$_3$ thin films was characterized by atomic force microscope (Flex-Axiom, Nanosurf) and $\theta-2\theta$ x-ray diffraction patterns were taken with the Cu K$_\alpha$ radiation ($\lambda = 1.54$ Å) at a scanning rate of 2 deg. per minute using Rigaku MiniFlex 600. Similarly, we measured near normal-incidence transmittance and reflectance with a spectral resolution of 1 nm, using a dual-beam spectrophotometer (Perkin Elmer Lambda 950). The magnetic moment as function of temperature and magnetic field were measured using a vibrating sample magnetometer (9 Tesla PPMS, Dynacool, Quantum Design).

3. Results and discussion

Fig. 1 shows the θ - 2θ x-ray diffraction (XRD) patterns of ~150 nm h-HoFeO$_3$ thin films deposited on (001) Al$_2$O$_3$ single crystal substrate at three different temperatures. These thin films were deposited in the oxygen and argon partial pressures of 0.27 Pa, and all samples were post-deposition annealed at 800 °C in air. The XRD pattern of the film deposited at 750 °C shows that the film is amorphous without any visible peaks from the sample. On the other hand, the films deposited at 800 and 825 °C show the multiple c-plane peaks from h-HoFeO$_3$. The XRD pattern of the h-HoFeO$_3$/Al$_2$O$_3$ film at 825 °C shows four peaks at 15.1°, 29.7°, 52°, and 61.8° corresponding to the (002), (004), (006), and (008)
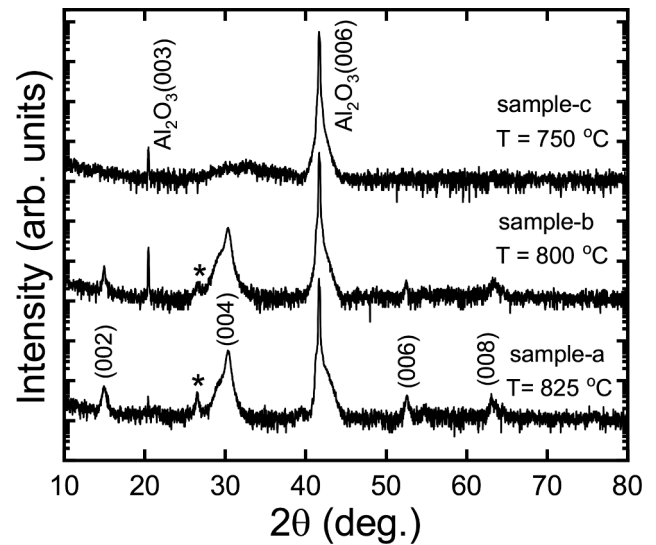

Fig. 1. The XRD patterns of 150 nm h-HoFeO$_3$ thin films deposited on (001) Al$_2$O$_3$ at 750, 800, and 825 °C and annealed at 800 °C. Mostly the (00l) planes are observed, indicating the hexagonal phase of HoFeO$_3$. A weak peak at ~ 27° (marked by *) for the film annealed at 800 °C and 825 °C is due to an ortho-rhombic phase of HoFeO$_3$.

planes of h-HoFeO$_3$, respectively. These XRD patterns confirm a hexagonal phase of HoFeO$_3$ thin films. Using the XRD data, the lattice constant is found to be $c = 12.02$ Å, consistent with the reported value in the literature [3,27]. A weak peak at ~ 27° (represented by * for sample-a and sample-b) is most likely from the orthorhombic phase of HoFeO$_3$. Similarly, a sharp peak at ~ 20° in all three XRD patterns corresponds to the (003) plane of Al$_2$O$_3$. Therefore, the XRD patterns confirm the c-plane textured h-HoFeO$_3$/Al$_2$O$_3$ thin film with a small fraction of the orthorhombic-HoFeO$_3$ (o-HoFeO$_3$) impurity phase. All the presented data here were measured on sample-a, h-HoFeO$_3$/Al$_2$O$_3$ film deposited at 825 °C.

In order to identify the elements in the sample, we carried out the energy-dispersive x-ray (EDX) analysis using Scanning Electron Microscope (SEM). Fig. 2(a) shows an EDX spectrum of an h-HoFeO$_3$/Al$_2$O$_3$ film which was annealed at 825 °C. The EDX data, as shown in the inset, correctly identified all the expected elemental peaks. The spectrum also shows 0.2% of argon as impurities. Since argon gas was used for sputtering the source target, its presence in a small amount like this was not surprising. As shown in the inset table of Fig. 2(a), all the elements were detected. Note that the observed aluminum peak comes from the substrate (Al$_2$O$_3$). We also studied the surface morphology of the thin films. Fig. 2(b) and (c) show representative (4m x 4m and 1m x 1m) atomic force microscope (AFM) images which were taken at room temperature in the non-contact tapping mode. While most of the scanned film area showed a smooth surface with granular structures, there were areas such as shown in Fig. 2(b) where the domain like structures were separated by some fault lines. As shown in Fig. 2(c), a close-up view of the film surface in a smooth region away from the fault lines (indicated by the white dash lines in Fig. 2(b)), shows a relatively smooth surface with granular structures of the sizes between ~100 nm and ~200 nm. The surface roughness root-mean-squared values were typically on the order of 5 nm.

Fig. 3 (a) shows room temperature transmittance and reflectance of the h-HoFeO$_3$/Al$_2$O$_3$ thin film as a function of wavelength. The transmittance represents the ratio between the film-substrate intensity and the bare substrate intensity which were simultaneously measured in a dual-beam spectrophotometer. For the reflectance, an aluminum mirror was used to measure the reference signal and the aluminum feature has been corrected. Room temperature absorption coefficient (α) versus photon energy, as shown in Fig. 3 (b), was calculated using
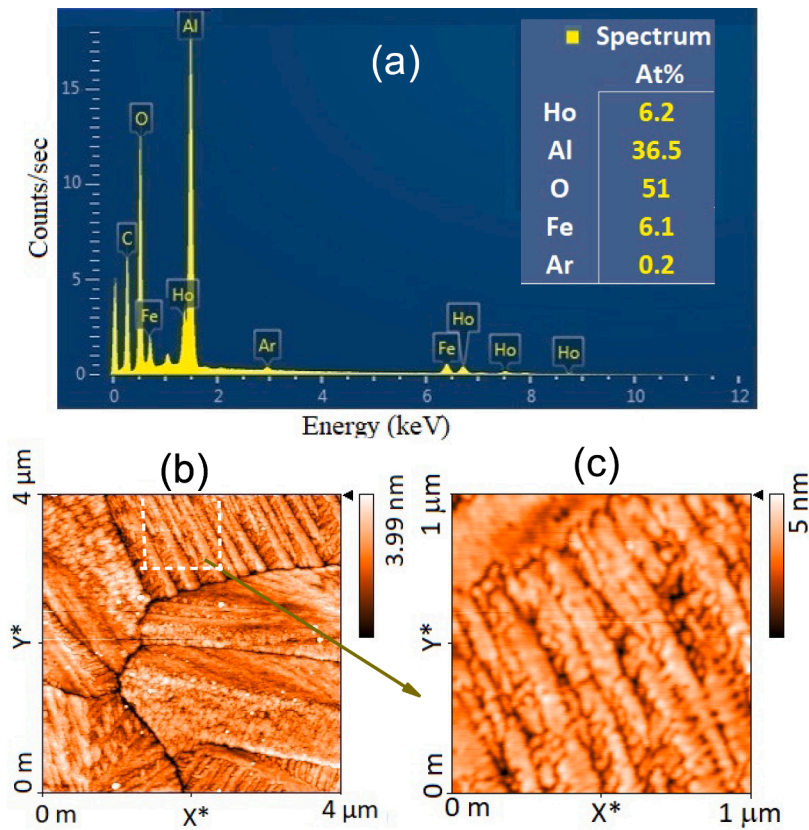
Fig. 2. (a) An EDX spectrum of the h-HoFeO$_3$/Al$_2$O$_3$ film. The elemental composition, as shown in the inset, confirms HoFeO$_3$. AFM images, (b) 4m x 4m and (c) 1m x 1m, show the z-axis surface morphology of h-HoFeO$_3$/Al$_2$O$_3$ film. The scan was done in the dynamic force mode.
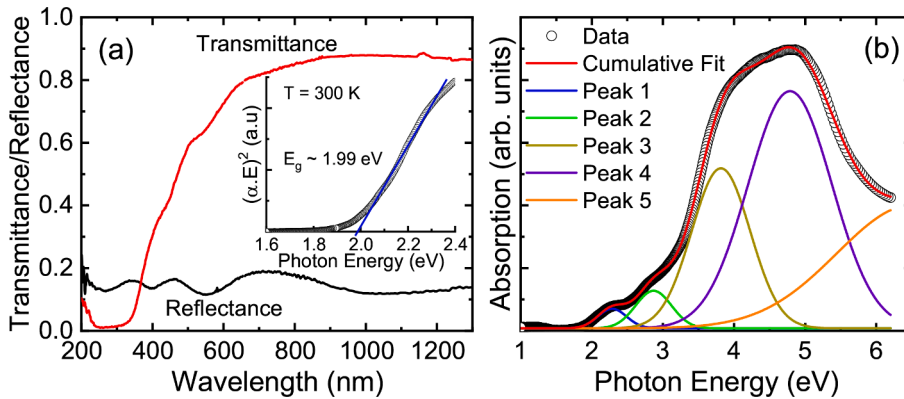

Fig. 3. (a) Room temperature reflectance and transmittance as a function of wavelength for the h-HoFeO$_3$/Al$_2$O$_3$ thin film. The inset shows the extraction of the direct energy band gap of h-HoFeO$_3$ from the $(\alpha \cdot E)^2$ versus photon energy. (b) Absorption coefficient as a function of photon energy for the h-HoFeO$_3$/Al$_2$O$_3$ thin film, extracted from a simultaneous fitting of the reflectance and transmittance data. The solid lines represent the multi-peak fitting to find out the electronic excitations in the spectrum.

$\alpha = -(1/d)\ln[t/(1-r)]$, where d is the film thickness, "t" is the transmittance, and "r" is the reflectance. Then, the absorption spectrum was fitted with the Gaussian-amplitude function to identify the electronic transitions. The best fit (red solid line) was obtained with 5 peaks at ~2.29, 2.87, 3.82, 4.79, and 6.53 eV, as indicated by the color solid lines. Based on the theoretical calculations and comparison with the experimental data for h-LuFeO$_3$/Al$_2$O$_3$ thin films [4,5,12,26,28], we assigned the electronic excitations at 2.29 eV to Fe^{3+} d to d on-site, 2.87 and 3.82 eV to O $2p$ to Fe $3d$ charge-transfer, and 4.79 and 6.53 eV to O $2p$ to Ho $6s$ and $5d$ charge-transfer electronic transitions. In the h-RFeO$_3$ system, the structural building block is a trigonal bipyramidal FeO$_5$ and the O $2p$ and Fe $3d$ states are hybridized in the system, relaxing the Fe d to d transition. As a result, the observed electronic excitations for h-HoFeO$_3$ are consistent with the crystal-field environment in FeO$_5$. Further, the electronic excitations of h-HoFeO$_3$ are very similar to

isostructural h-LuFeO$_3$ and h-YbFeO$_3$ [4,5,12,26,28–30]. Finally, the energy band gap of the h-HoFeO$_3$ thin film has been extracted by fitting the absorption with the direct energy band gap model. The fitting, as shown in the inset of Fig. 3a, gives the room temperature energy gap to be ~1.99 ± 0.04 eV. This energy gap of 1.98 eV is comparable to the energy gaps of h-YbFeO$_3$ and h-LuFeO$_3$ thin films [5,28–30].

To study the magnetic properties of the h-HoFeO$_3$ thin film, we measured the temperature (T) dependence of zero-field cooled (ZFC) cooling and field-cooled (FC) warming magnetic moments (M) with 80 kA/m and 400 kA/m fields (H) in the out-of-plane (H∥c-axis) and in-plane (H⊥c-axis) directions, as shown in Fig. 4(a, b, c, & d), respectively. For both ZFC cooling and FC warming runs, the data were taken with the sample cooling/warming rate of 2 K/minute. The substrate contributions to the moment have been subtracted from the data. At 80 kA/m field for both H∥c and H⊥c directions, the M-T curves show a

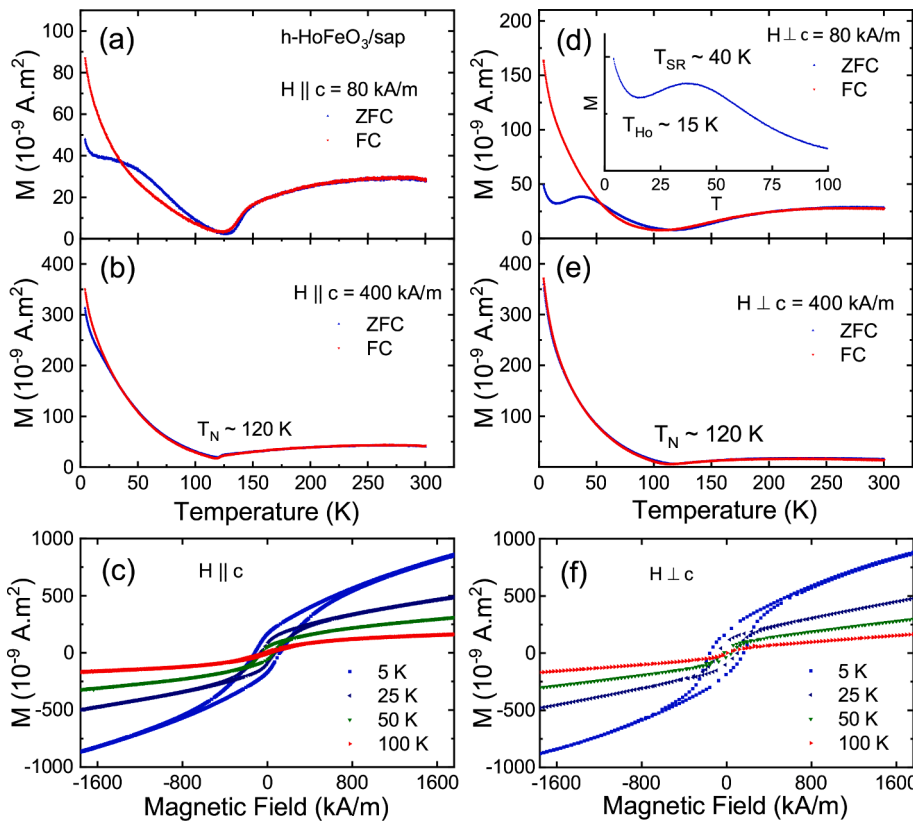**Fig. 4.** The ZFC and FC magnetic moment (M) for a h-HoFeO$_3$/Al$_2$O$_3$ thin film as a function of temperature for (a)-(b) the out-of-plane (H‖c-axis) fields at 80 kA/m and 400 kA/m and (d)-(e) the in-plane (H⊥c-axis) fields at 80 kA/m and 400 kA/m, respectively. The broad peak at ∼40 K in the ZFC data, as highlighted in the inset of (d), indicates the Fe^{3+} spin reorientation transition due to the interactions between Ho^{3+} and Fe^{3+} spins. The out-of-plane (c) and in-plane (f) M-H hysteresis loops for a h-HoFeO$_3$/Al$_2$O$_3$ thin film at 5, 25, 50, and 100 K, respectively. The existence of M-H loops below T$_N$ is consistent with a weak ferromagnetism due to a canted spin structure in the system.

broad magnetic transition around 120 K. As shown in Fig. 4(b) and (e), however, the M-T curves with 400 kA/m show a sharp long-range antiferromagnetic transition at T$_N$ ∼120 ± 5 K, which is consistent with the previously reported T$_N$ for h-HoFeO$_3$ [13,26]. It is clear that the transition temperature is relatively sharper for H‖c for both 80 & 400 kA/m fields. This is consistent with the fact that the Fe^{3+} spins are expected to be canted out of the *ab* plane.

Comparing the M-T curves in Fig. 4(a, b, c, & d), it is evident that the in-plane moments are comparable to the out-of-plane moments for both 80 kA/m and 400 kA/m fields. In the h-RFeO$_3$ family, the Fe^{3+} spins are aligned in a 120° triangular spin structure on the *ab* plane with a spin canting along the *c* axis due to the Dzyaloshinskii-Moriya interaction (Γ$_2$ spin structure) [4,7,12,14]. That means, the out-of-plane moments should be stronger than the in-plane moments for the Fe^{3+} ions. However, the measured moments at low temperatures were not only from the Fe^{3+} sites, but the contribution from the Ho^{3+} (4f^{10}) ions should also be taken into account in this system. Therefore, the low temperature moments of h-HoFeO$_3$ come from both Fe^{3+} ions and Ho^{3+} ions.

The ZFC M-T curves at 80 kA/m for both H‖c and H⊥c, as shown in Fig. 4(a & d), have a broad peak at ∼40 K, likely indicating a spin reorientation transition in which some of the Fe^{3+} moments rotate by 90° in the *ab* plane, thus changing the magnetic symmetry. It is believed that the spin reorientation in h-HoFeO$_3$ is caused by the magnetic superexchange interactions between the Ho^{3+} and Fe^{3+} ions [4,7]. There have been reports of the spin reorientation transition in other h-RFeO$_3$ members as well [9,14,25]. The neutron scattering data on h-LuFeO$_3$ suggest that the magnetic structure is a mixed Γ$_1$ + Γ$_2$ state after the spin reorientation transition [14,31]. While the canted antiferromangetic moment of the Fe^{3+} ions along the *c* direction becomes smaller in this mixed state, the in-plane moment is no longer insignificant. The observed magnetization data Fig. 4(a, b, c, & d), having comparable values in both directions support the mixed magnetic structure. Additionally, the spin reorientation transition has also been

reported for isostructural hexagonal manganite like HoMnO$_3$ [32–34]. Given that the magnetic structures of h-HoFeO$_3$ and h-HoMnO$_3$ are similar, the spin reorientation phenomenon in both compounds could be directly related.

On the other hand, the ZFC and FC magnetic moments increase rapidly below T$_N$, mainly due to the emergence of the Ho^{3+} moments. At 400 kA/m, the magnetic moment has a significant contribution from the Ho^{3+} ions, thus masking the Fe^{3+} spin orientation peak. In addition, the Ho^{3+} moments are expected to magnetically order at low temperature. As shown in Fig. 4(a) and (d), the ZFC moment gradually increases below 15 K, as indicated by an upturn. Therefore, the M-T data suggest that the Ho^{3+} spins order below ∼15 K in h-HoFeO$_3$. Based on the theoretical calculations, the Ho^{3+} spins are aligned antiferromagnetically along the *c* directions and ferri/ferromagnetically in the *ab* plane [4,20,33]. In h-HoFeO$_3$, the Ho^{3+} moments are aligned by the magnetic field of the Fe^{3+} sites through the Fe^{3+}- Ho^{3+} interactions. As a result, the Ho^{3+} sites significantly contribute to the overall magnetic moments in both directions at low temperature. Similar upturn in the M-T data has also been observed in h-YbFeO$_3$ samples caused by the ordering of the Yb^{3+} spins [3,20,23,29].

Fig. 4 (c) display the M-H hysteresis loops for H‖c below 100 K, indicating the existence of a weak ferromagnetism due to spin canting along the *c* axis. We measured the coercive field for the h-HoFeO$_3$ thin film at 5 K to be 320 kA/m. We also observed the hysteresis effects for the in-plane fields [Fig. 4(f)], providing further evidence for the mixed magnetic structure driven by the Fe^{3+}- Ho^{3+} interactions. In both directions, the 5 K loops have the saturation fields of about 800 kA/m. The hysteresis loop decreases in size at high temperature and disappears around T$_N$. It is evident that the M-H loop at 100 K is very small for H‖c whereas it is nonexistent for H⊥c, which is consistent with the fact that the high temperature moments are mainly due to the Fe^{3+} spins.

4. Conclusions

We deposited h-HoFeO$_3$ thin films on *c*-axis Al$_2$O$_3$ substrates by RF magnetron sputtering. The x-ray diffraction spectrum of the h-HoFeO$_3$ thin film deposited at 825 °C shows the c-planes of a hexagonal structure. The temperature dependence of the mangetic moment displays the long-range magnetic ordering at T$_N$ ∼120 ± 5 K. The ZFC magnetization measured at 80 kA/m shows an anomaly around ∼40 K, indicating a spin-reorientation transition caused by the Ho^{3+}- Fe^{3+} interactions. The M-H hysteresis loops have been observed below 100 K, confirming a weak ferromagnetism arising from canting of the Fe^{3+} spins out of the *ab* plane. Below 40 K, the Ho^{3+} ions contribute significantly to the complex magnetic properties of h-HoFeO$_3$. The room temperature absorption spectrum in the UV–vis range shows several electronic transitions above the energy band gap of ∼1.99 ± 0.04 eV.

CRediT authorship contribution statement

R.C. Rai: Conceptualization, Data curation, Formal analysis, Investigation, Methodology, Software, Writing - original draft, Writing - review & editing. **C. Horvatits:** Conceptualization, Data curation, Formal analysis, Investigation, Methodology, Software, Writing - original draft, Writing - review & editing. **S. Deer:** Conceptualization, Data curation, Formal analysis, Investigation, Methodology, Software, Writing - original draft, Writing - review & editing.

Declaration of Competing Interest

The authors declare that they have no known competing financial interests or personal relationships that could have appeared to influence the work reported in this paper.

Acknowledgments

Supplementary material

Supplementary material associated with this article can be found, in the online version, at 10.1016/j.tsf.2021.138596

References

[1] A.A. Bossak, I.E. Graboy, O.Y. Gorbenko, A.R. Kaul, M.S. Kartavtseva, V. L. Svetchnikov, H.W. Zandbergen, Xrd and hrem studies of epitaxially stabilized hexagonal orthoferrites RFeO$_3$ (R = Eu-Lu), Chem. Mater. 16 (9) (2004) 1751–1755, https://doi.org/10.1021/cm0353660.

[2] A. Masuno, S. Sakai, Y. Arai, H. Tomioka, F. Otsubo, H. Inoue, C. Moriyoshi, Y. Kuroiwa, J.D. Yu, Structure and physical properties of metastable hexagonal LuFeO$_3$, Ferroelectrics 378 (2009) 169–174, https://doi.org/10.1080/00150190902848719.

[3] H. Iida, T. Koizumi, Y. Uesu, K. Kohn, N. Ikeda, S. Mori, R. Haumont, P.-E. Janolin, J.-M. Kiat, M. Fukunaga, Y. Noda, Ferroelectricity and ferrimagnetism of hexagonal YbFeO$_3$ thin films, J. Phys. Soc. Japan 81 (2) (2012) 024719, https://doi.org/10.1143/JPSJ.81.024719.

[4] S.J. Ahn, J.H. Lee, H.M. Jang, Y.K. Jeong, Multiferroism in hexagonally stabilized TmFeO$_3$ thin films below 120 k, J. Mater. Chem. C 2 (23) (2014) 4521–4525, https://doi.org/10.1039/C4TC00461B.

[5] W. Wang, H. Wang, X. Xu, L. Zhu, L. He, E. Wills, X. Cheng, D.J. Keavney, J. Shen, X. Wu, X. Xu, Crystal field splitting and optical bandgap of hexagonal LuFeO$_3$ films, Appl. Phys. Lett. 101 (24) (2012) 241907, https://doi.org/10.1063/1.4771601.

[6] A.R. Akbashev, V.V. Roddatis, A.L. Vasiliev, S. Lopatin, V.A. Amelichev, A.R. Kaul, Reconstruction of the polar interface between hexagonal LuFeO$_3$ and intergrown fe$_3$o$_4$ nanolayers, Sci. Rep. (2012) 672, https://doi.org/10.1038/srep00672.

[7] X.S. Xu, W.B. Wang, Multiferroic hexagonal ferrites (h-RFeO$_3$, R = Y, Dy-Lu): a brief experimental review, Mod. Phys. Lett. B 28 (21) (2014) 1430008, https://doi.org/10.1142/S0217984914300087.

[8] H. Yokota, T. Nozue, S. Nakamura, H. Hojo, M. Fukunaga, P.E. Janolin, J.M. Kiat, A. Fuwa, Ferroelectricity and weak ferromagnetism of hexagonal ErFeO$_3$ thin films, Phys. Rev. B 92 (5) (2015) 054101, https://doi.org/10.1103/PhysRevB.92.054101.

[9] L. Lin, H.M. Zhang, M.F. Liu, S. Shen, S. Zhou, D. Li, X. Wang, Z.B. Yan, Z.D. Zhang, J. Zhao, S. Dong, J.M. Liu, Hexagonal phase stabilization and magnetic orders of multiferroic Lu$_{1−x}$Sc$_x$FeO$_3$, Phys. Rev. B 93 (7) (2016) 075146, https://doi.org/10.1103/PhysRevB.93.075146.

[10] K. Sinha, H. Wang, X. Wang, L. Zhou, Y. Yin, W. Wang, X. Cheng, D.J. Keavney, H. Cao, Y. Liu, X. Wu, X. Xu, Tuning the néel temperature of hexagonal ferrites by structural distortion, Phys. Rev. Lett. 121 (2018) 237203, https://doi.org/10.1103/PhysRevLett.121.237203.

[11] J.A. Mundy, C.M. Brooks, M.E. Holtz, J.A. Moyer, H. Das, A.F. Rébola, J.T. Heron, J.D. Clarkson, S.M. Disseler, Z. Liu, A. Farhan, R. Held, R. Hovden, E. Padgett, Q. Mao, H. Paik, R. Misra, L.F. Kourkoutis, E. Arenholz, A. Scholl, J.A. Borchers, W. D. Ratcliff, R. Ramesh, C.J. Fennie, P. Schiffer, D.A. Muller, D.G. Schlom, Atomically engineered ferroic layers yield a room - temperature magnetoelectric multiferroic, Nature 537 (7621) (2016) 523, https://doi.org/10.1038/nature19343.

[12] Y.K. Jeong, J.-H. Lee, S.-J. Ahn, H.M. Jang, Epitaxially constrained hexagonal ferroelectricity and canted triangular spin order in LuFeO$_3$ thin films, Chem. Mater. 24 (13) (2012) 2426–2428, https://doi.org/10.1021/cm300846j.

[13] A. Akbashev, A. Semisalova, N. Perov, A. Kaul, Weak ferromagnetism in hexagonal orthoferrites RFeO$_3$ (R= Lu, Er-Tb), Appl. Phys. Lett. 99 (12) (2011) 122502, https://doi.org/10.1063/1.3643043.

[14] S.M. Disseler, J.A. Borchers, C.M. Brooks, J.A. Mundy, J.A. Moyer, D.A. Hillsberry, E.L. Thies, D.A. Tenne, J. Heron, M.E. Holtz, J.D. Clarkson, G.M. Stiehl, P. Schiffer, D.A. Muller, D.G. Schlom, W.D. Ratcliff, Magnetic structure and ordering of multiferroic hexagonal LuFeO$_3$, Phys. Rev. Lett. 114 (21) (2015) 217602, https://doi.org/10.1103/PhysRevLett.114.217602.

[15] W.K. Zhu, L. Pi, S. Tan, Y.H. Zhang, Anisotropy and extremely high coercivity in weak ferromagnetic LuFeO$_3$, Appl. Phys. Lett. 100 (5) (2012) 052407, https://doi.org/10.1063/1.3681789.

[16] S. Cao, X. Zhang, T.R. Paudel, K. Sinha, X. Wang, X. Jiang, W. Wang, S. Brutsche, J. Wang, P.J. Ryan, J.-W. Kim, X. Cheng, E.Y. Tsymbal, P.A. Dowben, X. Xu, On the structural origin of the single-ion magnetic anisotropy in LuFeO$_3$, J. Phys. Condens. Matter 28 (15) (2016) 156001, https://doi.org/10.1088/0953-8984/28/15/156001.

[17] M.V. Kumar, K. Kuribayashi, K. Nagashio, T. Ishikawa, J. Okada, J. Yu, S. Yoda, Y. Katayama, Real-time x-ray diffraction of metastable phases during solidification from the undercooled lufeo$_3$ melt by two-dimensional detector at 1 khz, Appl. Phys. Lett. 100 (19) (2012) 191905, https://doi.org/10.1063/1.4712124.

[18] J.A. Moyer, R. Misra, J.A. Mundy, C.M. Brooks, J.T. Heron, D.A. Muller, D. G. Schlom, P. Schiffer, Intrinsic magnetic properties of hexagonal LuFeO$_3$ and the effects of nonstoichiometry, APL Mater 2 (1) (2014) 012106, https://doi.org/10.1063/1.4861795.

[19] S.M. Disseler, X. Luo, B. Gao, Y.S. Oh, R. Hu, Y. Wang, D. Quintana, A. Zhang, Q. Huang, J. Lau, R. Paul, J.W. Lynn, S.-W. Cheong, W. Ratcliff, Multiferroicity in doped hexagonal LuFeO$_3$, Phys. Rev. B 92 (2015) 054435, https://doi.org/10.1103/PhysRevB.92.054435.

[20] Y.K. Jeong, J.-H. Lee, S.-J. Ahn, S.-W. Song, H.M. Jang, H. Choi, J.F. Scott, Structurally tailored hexagonal ferroelectricity and multiferroism in epitaxial ybfeo$_3$ thin-film heterostructures, J. Am. Chem. Soc. 134 (3) (2012) 1450–1453, https://doi.org/10.1021/ja210341b.

[21] W. Wang, J.A. Mundy, C.M. Brooks, J.A. Moyer, M.E. Holtz, D.A. Muller, D. G. Schlom, W. Wu, Visualizing weak ferromagnetic domains in multiferroic hexagonal ferrite thin film, Phys. Rev. B 95 (2017) 134443, https://doi.org/10.1103/PhysRevB.95.134443.

[22] K. Sinha, Y. Zhang, X. Jiang, H. Wang, X. Wang, X. Zhang, P.J. Ryan, J.-W. Kim, J. Bowlan, D.A. Yarotski, Y. Li, A.D.D. Chiara, X. Cheng, X. Wu, X. Xu, Effects of biaxial strain on the improper multiferroicity in *h* − LuFeo$_3$ films studied using the restrained thermal expansion method, Phys. Rev. B 95 (2017) 094110, https://doi.org/10.1103/PhysRevB.95.094110.

[23] S. Cao, K. Sinha, X. Zhang, X. Zhang, X. Wang, Y. Yin, A.T. N`Diaye, J. Wang, D. J. Keavney, T.R. Paudel, Y. Liu, X. Cheng, E.Y. Tsymbal, P.A. Dowben, X. Xu, Electronic structure and direct observation of ferrimagnetism in multiferroic hexagonal ybfeo$_3$, Phys. Rev. B 95 (22) (2017) 224428, https://doi.org/10.1103/PhysRevB.95.224428.

[24] K. Du, B. Gao, Y. Wang, X. Xu, J. Kim, R. Hu, F.-T. Huang, S.W. Cheong, Vortex ferroelectric domains, large-loop weak ferromagnetic domains, and their decoupling in hexagonal (lu, sc)FeO$_3$, npj Quantum Mater. 3 (1) (2018) 33, https://doi.org/10.1038/s41535-018-0106-3.

[25] A. Masuno, A. Ishimoto, C. Moriyoshi, H. Kawaji, Y. Kuroiwa, H. Inoue, Expansion of the hexagonal phase-forming region of Lu$_{1−x}$Sc$_x$FeO$_3$ by container less processing, Inorg. Chem. 54 (19) (2015) 9432–9437, https://doi.org/10.1021/acs.inorgchem.5b01225.

[26] V.V. Pavlov, A.R. Akbashev, A.M. Kalashnikova, V.A. Rusakov, A.R. Kaul, M. Bayer, R.V. Pisarev, Optical properties and electronic structure of multiferroic hexagonal orthoferrites RFeo$_3$ (r = ho, er, lu), J. Appl. Phys. 111 (5) (2012) 056105, https://doi.org/10.1063/1.3693588.

[27] X. Zhang, Y. Yin, S. Yang, Z. Yang, X. Xu, Effect of interface on epitaxy and magnetism in h-RFeO$_3$/Fe$_3$O$_4$/Al$_2$O$_3$ films (r = lu, yb), J. Phys. Condens. Matter 29 (16) (2017) 164001, https://doi.org/10.1088/1361-648X/aa5fec.

[28] B.S. Holinsworth, D. Mazumdar, C.M. Brooks, J.A. Mundy, H. Das, J.G. Cherian, S. A.M. Gill, C.J. Fennie, D.G. Schlom, J.L. Musfeldt, Direct band gaps in multiferroic h-LuFeO$_3$, Appl. Phys. Lett. 106 (8) (2015) 082902, https://doi.org/10.1063/1.4908246.

[29] R.C. Rai, C. Horvatits, D. Mckenna, J.D. Hart, Structural studies and physical properties of hexagonal-YbFeO$_3$ thin films, AIP Adv 9 (1) (2019) 015019, https://doi.org/10.1063/1.5027094.

[30] R.C. Rai, D. Mckenna, C. Horvatits, J. Du, Annealing induced structural phase change of hexagonal-LuFeO$_3$ thin films, John Wiley & Sons, Ltd, 2018, https://doi.org/10.1002/9781119494096.ch21.Ch. 21

[31] W. Wang, J. Zhao, W. Wang, Z. Gai, N. Balke, M. Chi, H.N. Lee, W. Tian, L. Zhu, X. Cheng, D.J. Keavney, J. Yi, T.Z. Ward, P.C. Snijders, H.M. Christen, W. Wu, J. Shen, X. Xu, Room-temperature multiferroic hexagonal lufeo$_3$ films, Phys. Rev. Lett. 110 (2013) 237601, https://doi.org/10.1103/PhysRevLett.110.237601.

[32] A. Munoz, J.A. Alonso, M.J. Martínez-Lope, M.T. Casáis, J.L. Martínez, M.T. Fernández-Díaz, Evolution of the magnetic structure of hexagonal HoMNo$_3$ from neutron powder diffraction data, Chem. Mater. 13 (5) (2001) 1497–1505, https://doi.org/10.1021/cm0012264.

[33] T. Lottermoser, T. Lonkai, U. Amann, D. Hohlwein, J. Ihringer, M. Fiebig, Magnetic phase control by an electric field, Nature 430 (6999) (2004) 541, https://doi.org/10.1038/nature02728.

[34] O. Vajk, M. Kenzelmann, J. Lynn, S. Kim, S.W. Cheong, Magnetic order and spin dynamics in ferroelectric HoMnO$_3$, Phys. Rev. Lett. 94 (8) (2005) 087601, https://doi.org/10.1103/PhysRevLett.94.087601.